Gridless One-Bit Direction-of-Arrival Estimation via Atomic Norm Denoising

Zhenyu Wei, *Student Member, IEEE*, Wei Wang, *Senior Member, IEEE*, Fuwang Dong, and Qi Liu, *Member, IEEE*

***Abstract*— In this letter, a gridless one-bit direction-of-arrival (DOA) estimation approach with one-snapshot is proposed to be robust against the off-grid errors and sign inconsistency because of the one-bit measurements corrupted by additive noise. Different with the existing off-grid DOA estimators, an atomic norm minimization is considered to mitigate the grid mismatch with atoms instead of pre-divided discretized dictionary. Then, the sign inconsistency of one-bit measurements is solved by introducing a linear loss function. The resulting optimization problem is convex and can be equivalent to a semidefinite programming (SDP) problem, which, however, is computational demanding. Therefore, alternating direction multiplier method (ADMM) is employed to speed up the implementation. To avoid the spectrum searching, an effective dual polynomial method is developed with closed-form solution for DOA estimation. Meanwhile, the proposed method does not require $a\ prior$ information of the number of targets. Simulation results demonstrate the superiority and effectiveness of the proposed method.**

***Index Terms*— Atomic norm minimization, gridless direction-of-arrival (DOA) estimation, one-bit quantization, alternating direction multiplier method (ADMM), sparse recovery.**

I. Introduction

FINDING directions of multiple targets with massive antenna array is an essential task since its merits of high spatial resolution and high spectral efficiency are required in various applications, ranging from sonar, radar, wireless communication and navigation [1]–[5]. However, it is inefficient for analog-to-digital converters (ADC) during the procedures of quantization and sampling, as the result of power consumption growing exponentially with sampling bit-depth. Therefore, how to reduce the hardware complexity becomes fertile research ground that merits further investigation especially in massive antenna array systems.

Recently, one-bit quantization becomes an emerging technology that is attracting the attentions of researchers and practitioners alike. On the basis of that, the power consumption of one-bit measurements is significantly reduced. Although only sign information of the measurements is available after one-bit quantization, it has been demonstrated that robust direction-of-arrival (DOA) estimation can still be guaranteed [6], [7]. In [6], one-bit MUSIC is proposed based on quantized array measurements. In [7], to resolve more sources than the number of antennas, sparse linear array (SLA) is considered for DOA estimation with one-bit quantization. Nevertheless, these one-bit DOA estimation algorithms still require relatively large number of snapshots to reconstruct the covariance matrix.

On the other hand, benefit from compressed sensing (CS), sparse recovery-based DOA estimators perform better performance with limit snapshots or even one snapshot, including fixed-point continuation (FPC) [8] and binary iterative hard threshold (BIHT) [9]. In [10], the BIHT algorithm is extended to complexed-valued model for DOA estimation, referred to complex-valued BIHT (CBIHT). By exploiting the similarities between one-bit sparse recovery model and classification problem, a novel one-bit classification model is established, where support vector machine (SVM) is utilized to extract the DOA information [11]. In addition, Huang *et al.* [12] proposed an improved FPC reconstruction algorithm for DOA estimation. In [13], a generalized sparse Bayesian learning algorithm (Gr-SBL) is developed for DOA estimation. Nevertheless, these one-bit DOA estimators always require a pre-defined discretized spatial dictionary to estimate DOAs, under the assumption of targets exactly corresponding to the discretized dictionary grids. In practical scenarios, the target positions are not precisely on the grids and thus DOA estimation bias exists, leading to significant degradation performance. To deal with off-grid error, several gridless methods are proposed for DOA estimation with one-bit measurements [14], [15]. However, during the procedures of sampling and transmission, the sign inconsistency between the measurements before and after one-bit quantization has a further negative effect on the estimation accuracy because of the noise.

In this letter, a robust gridless DOA estimator with one-snapshot is developed on the massive SLA. To achieve the gridless DOA estimation, a sparse reconstruction model with one-bit quantization is built based on the atomic norm minimization. Then, a linear loss function is exploited to constrain the sign inconsistency between the one-bit measurements and the ground-truth signals. Due to the convexness of the semidefinite programming (SDP) optimization problem, it can be tackled by interior-point methods or SDP solvers. Still, it is time-consuming, and alternating direction multiplier (ADMM) is then applied as the efficient solver. Finally, to avoid the spectrum searching, an effective dual polynomial method is designed for DOA estimation with closed-form solution.

The main contributions are categorized as follows, 1) A novel one-bit quantized model based on atomic norm

Manuscript received May 9, 2020; accepted June 4, 2020. Date of publication June 8, 2020; date of current version October 9, 2020. The work was supported in part by the National Natural Science Foundation (61871143), Fundamental Research for the Central University (HEUCFP201836), Heilongjiang Natural Science Foundation (LH2019F006) and Research and Development Project of Application Technology in Harbin (2017R-AQXJ095). The associate editor coordinating the review of this letter and approving it for publication was M. Egan. *(Corresponding authors: Wei Wang; Qi Liu.)*

Zhenyu Wei, Wei Wang, and Fuwang Dong are with the College of Automation, Harbin Engineering University, Harbin 150001, China (e-mail: wangwei407@hrbeu.edu.cn).

Qi Liu is with the Department of Electrical and Computer Engineering, National University of Singapore, Singapore 117583 (e-mail: elelqi@nus.edu.sg).

Digital Object Identifier 10.1109/LCOMM.2020.3000755

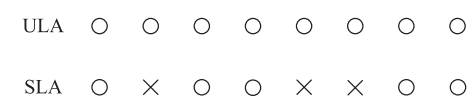

Fig. 1. An illustration of ULA and SLA, where the circles and crosses represent sensors and holes, respectively. There are eight sensor elements in the ULA while the SLA has the same antenna aperture as ULA with only five sensors.

minimization is built for DOA estimation, where the off-grid and sign inconsistency problems are addressed. 2) The resulting optimization problem is equivalently transformed to SDP problem, however, it is not computational friendly. Therefore, ADMM method is adopted as the efficient solver. 3) A dual polynomial method with closed-form solution is proposed to avoid the spectrum searching without requiring $a\ prior$ information of source number.

II. Signal Model With One-Bit Quantization

Consider a massive uniform linear array (ULA) system with N omnidirectional antennas, where the inter-spacing of sensors is d. Assume that K narrowband far-field and uncorrelated sources impinge on the ULA from directions $\{\theta_1, \theta_2, \ldots, \theta_K\}$, with $\theta_k \in [-\pi/2, \pi/2]$. Note that the noise-free signal model of the massive ULA system at one snapshot is expressed as,

$$\mathbf{p} = \mathbf{A}\mathbf{s}, \tag{1}$$

where $\mathbf{p} = [p_1, \ldots, p_N]^T \in \mathbb{C}^N$ and $\mathbf{s} = [s_1, s_2, \ldots, s_K]^T \in \mathbb{C}^K$ are the received signal vector without measurement noise and signal vector, respectively. $\mathbf{A} = [\mathbf{a}(\theta_1), \mathbf{a}(\theta_2), \ldots, \mathbf{a}(\theta_K)] \in \mathbb{C}^{N\times K}$ is the manifold matrix composed of the spatial steering vectors $\mathbf{a}(\theta_k) = [1, e^{j2\pi f_k}, \ldots, e^{j2\pi(N-1)\ f_k}]^T, k = 1, \ldots, K$, where $f_k = \frac{d}{\lambda}\sin\theta_k$ is the spatial angular frequency corresponding to θ_k with λ be the wavelength.

In general, some massive antenna array systems are configured with the SLA. The relation between ULA and SLA is illustrated in Fig. 1. To be specific, a real-valued selection matrix $\mathbf{\Gamma} \in \{0, 1\}^{M\times N}$ with only single 1 in each row is defined to model the SLA, where M is the number of sensors in the SLA. In the presence of noise, the signal model with SLA is modeled as [11],

$$\mathbf{x} = \mathbf{\Gamma}(\mathbf{p} + \mathbf{n}). \tag{2}$$

where $\mathbf{n} = [n_1, n_2, \ldots, n_N]^T \in \mathbb{C}^N$ is the Gaussian noise distribution with zero mean and variance σ_n^2.

To achieve low hardware complexity, one-bit quantization is considered. Then, (2) is modified as,

$$\mathbf{y} = \text{sign}(\Re\{\mathbf{x}\}) + j\text{sign}(\Im\{\mathbf{x}\}) \tag{3}$$

with one-bit measurements $\mathbf{y} \in \mathbb{C}^N$. $\Re\{\cdot\}$ and $\Im\{\cdot\}$ stand for the real and imaginary parts, respectively. Herein sign$(\cdot)$ is an element-wise function, defined as,

$$\text{sign}(v) = \begin{cases} 1, & \text{if } v \geq 0, \\ -1, & \text{if } v < 0. \end{cases} \tag{4}$$

As only sign information is available, the problem in (3) becomes more challenging for DOA estimation.

III. The Proposed Method

A. One-Bit Denoising Model With Atomic Norm

To deal with the off-grid problem, atomic norm is introduced. That is,

$$\|\mathbf{p}\|_{\mathcal{A}} = \inf_{c_k \geq 0} \{\sum_k c_k \mid \mathbf{p} = \sum_k c_k \mathbf{a}(f)\} \tag{5}$$

where $\mathcal{A}$ denotes the atomic set, defined as,

$$\mathcal{A} = \{\mathbf{a}(f), f = \frac{d}{\lambda}\sin\theta\}. \tag{6}$$

On the basis of that, $\mathbf{p}$ is sparsely represented by atoms in $\mathcal{A}$ instead of discretized dictionary. In the absence of noise, we have,

$$\Re\{\mathbf{y}\} \circ \Re\{\mathbf{\Gamma p}\} \geq 0, \tag{7}$$

$$\Im\{\mathbf{y}\} \circ \Im\{\mathbf{\Gamma p}\} \geq 0, \tag{8}$$

$$\|\Re\{\mathbf{\Gamma p}\}\|_1 + \|\Im\{\mathbf{\Gamma p}\}\|_1 = 1, \tag{9}$$

where $\circ$ denotes the hardmard product. These constrains ensure the sign consistency and enable that $\mathbf{p}$ can be exactly recovery on a unit sphere to avoid the trivial solutions. The loss function is commonly used to guarantee the data fidelity as well as to tolerate the existence of the sign inconsistence, with its simplicity and robust performance [16], [17]. Therefore, the problem in (3) can be solved by the following optimization,

$$\begin{aligned} \min_{\mathbf{p}} \ & -\frac{1}{2M}\begin{bmatrix}\Re\{\mathbf{\Gamma p}\}\\ \Im\{\mathbf{\Gamma p}\}\end{bmatrix}^T\begin{bmatrix}\Re\{\mathbf{y}\}\\ \Im\{\mathbf{y}\}\end{bmatrix} + \gamma\|\mathbf{p}\|_{\mathcal{A}} \\ \text{s.t. } & \|\Re\{\mathbf{\Gamma p}\}\|_1 + \|\Im\{\mathbf{\Gamma p}\}\|_1 \leq 1. \end{aligned} \tag{10}$$

where γ is the regularization parameter and the inequality equation in constraint is to ensure the convexness of (10) from (9). It is worth noting that the inequality equations (7) and (8) have emerged into the loss function in the above optimization problem. In addition, (10) can be seen as a denoising model compared with which used in [15].

Based on [18], [20], (10) can be equivalently transformed to a semidefinite programming (SDP) problem as,

$$\begin{aligned} \min_{\mathbf{p},\mathbf{u},t} \ & -\frac{1}{2M}\begin{bmatrix}\Re\{\mathbf{\Gamma p}\}\\ \Im\{\mathbf{\Gamma p}\}\end{bmatrix}^T\begin{bmatrix}\Re\{\mathbf{y}\}\\ \Im\{\mathbf{y}\}\end{bmatrix} + \gamma(t + u_1) \\ \text{s.t. } & \begin{bmatrix}\mathbf{T}(\mathbf{u}) & \mathbf{p}_R + j\mathbf{p}_I\\ (\mathbf{p}_R + j\mathbf{p}_I)^H & t\end{bmatrix} \geq 0, \\ & \|\mathbf{\Gamma p}_R\|_1 + \|\mathbf{\Gamma p}_I\|_1 \leq 1; \end{aligned} \tag{11}$$

where u_1 is the first element of $\mathbf{u}$. $\mathbf{T}(\mathbf{u})$ denotes a Toeplitz matrix with $\mathbf{u}$ as the first column. For brevity, we use $\mathbf{p}_R$ and $\mathbf{p}_I$ to represent the real and imaginary parts, respectively. The SDP problem can be tackled by the off-the-shelf tools [18], such as CVX and SeDuMi, which are not computational friendly.

B. Alternating Direction Method of Multipliers (ADMM) for One-Bit Denoising Model

In this section, to reduce the computational complexity, ADMM is utilized to speed up the implementation.

Before that, two auxiliary variables $\mathbf{Z}$ and α are introduced, and then (11) is modified as,

$$\begin{aligned}\min_{\mathbf{p}_R,\mathbf{p}_I,\mathbf{u},t} \quad & -\frac{1}{2M}(\mathbf{y}_R^T\mathbf{\Gamma}\mathbf{p}_R+\mathbf{y}_I^T\mathbf{\Gamma}\mathbf{p}_I)+\gamma(t+u_1)\\ \text{s.t. } \mathbf{Z}&=\begin{bmatrix}\mathbf{T}(\mathbf{u}) & \mathbf{p}_R+j\mathbf{p}_I\\ (\mathbf{p}_R+j\mathbf{p}_I)^H & t\end{bmatrix}\\ &\mathbf{Z}\geq 0\\ &\alpha=1-\mathbf{y}_R^T\mathbf{\Gamma}\mathbf{p}_R-\mathbf{y}_I^T\mathbf{\Gamma}\mathbf{p}_I\\ &\alpha\geq 0,\end{aligned} \tag{12}$$

where $\mathbf{y}_R=\Re\{\mathbf{y}\}$ and $\mathbf{y}_I=\Im\{\mathbf{y}\}$. Therefore, the augmented Lagrangian of (12) is written as,

$$\begin{aligned}&\mathcal{L}_\rho(\mathbf{p}_R,\mathbf{p}_I,\mathbf{u},t,\mathbf{Z},\mathbf{\Lambda},\alpha,\tau_\alpha)\\ &=-\frac{1}{2M}(\mathbf{y}_R^T\mathbf{\Gamma}\mathbf{p}_R+\mathbf{y}_I^T\mathbf{\Gamma}\mathbf{p}_I)+\gamma(t+u_1)\\ &\quad+\text{tr}\left\{\left(\mathbf{Z}-\begin{bmatrix}\mathbf{T}(\mathbf{u}) & \mathbf{p}_R+j\mathbf{p}_I\\ (\mathbf{p}_R+j\mathbf{x}_I)^H & t\end{bmatrix}\right)\mathbf{\Lambda}\right\}\\ &\quad+\frac{\rho}{2}\left\|\mathbf{Z}-\begin{bmatrix}\mathbf{T}(\mathbf{u}) & \mathbf{p}_R+j\mathbf{p}_I\\ (\mathbf{p}_R+j\mathbf{p}_I)^H & t\end{bmatrix}\right\|_F^2\\ &\quad+\tau_\alpha(\alpha-1+{\mathbf{y}_R}^T\mathbf{\Gamma}\mathbf{p}_R+{\mathbf{y}_I}^T\mathbf{\Gamma}\mathbf{p}_I)\\ &\quad+\frac{\rho}{2}\left\|\alpha-1+{\mathbf{y}_R}^T\mathbf{\Gamma}\mathbf{p}_R+{\mathbf{y}_I}^T\mathbf{\Gamma}\mathbf{p}_I\right\|_2^2.\end{aligned} \tag{13}$$

where $\rho>0$ is a penalty parameter. The ADMM consists of the following updating iterations,

$$\begin{aligned}&(\mathbf{p}_R^{l+1},\mathbf{p}_I^{l+1},t^{l+1},\mathbf{u}^{l+1})\\ &\quad=\arg\min_{\mathbf{p},t,\mathbf{u}}\mathcal{L}_\rho(\mathbf{p}_R,\mathbf{p}_I,t,\mathbf{u},\mathbf{Z}^l,\mathbf{\Lambda}^l,\alpha^l,\tau_\alpha^l),\end{aligned} \tag{14}$$

$$\begin{aligned}&(\mathbf{Z}^{l+1},\alpha^{l+1})\\ &\quad=\arg\min_{\mathbf{Z},\alpha}\mathcal{L}_\rho(\mathbf{p}_R^{l+1},\mathbf{p}_I^{l+1},t^{l+1},\mathbf{u}^{l+1},\mathbf{Z},\mathbf{\Lambda}^l,\alpha,\tau_\alpha^l),\end{aligned} \tag{15}$$

The sysmbol $(\cdot)^l$ denotes the estimates at l-th iteration. For the sake of convenience, $\mathbf{Z}$ and $\mathbf{\Lambda}$ are respectively partitioned as,

$$\mathbf{Z}=\begin{bmatrix}\mathbf{Z}_0 & \mathbf{z}_R+j\mathbf{z}_I\\ (\mathbf{z}_R+j\mathbf{z}_I)^H & z_{n+1,n+1}\end{bmatrix} \tag{16}$$

$$\mathbf{\Lambda}=\begin{bmatrix}\mathbf{\Lambda}_0 & \lambda_\mathbf{R}+j\lambda_\mathbf{I}\\ (\lambda_\mathbf{R}+j\lambda_\mathbf{I})^H & \Lambda_{n+1,n+1}\end{bmatrix} \tag{17}$$

with $\mathbf{Z}_0\in\mathbb{C}^{N\times N}$ and $\mathbf{\Lambda}_0\in\mathbb{C}^{N\times N}$. The updates with respect to the primal variables in (14) can be calculated via the following closed-form expressions,

$$\begin{cases}\mathbf{p}_R^{l+1}=(\rho+\frac{\rho}{2}\mathbf{b}_R^T\mathbf{b}_R)^{-1}(\frac{1}{4M}\mathbf{b}_R+\rho\mathbf{z}_R^l+\lambda_R^l+\frac{(\rho\alpha^l+\tau_\alpha^l)}{2}\mathbf{b}_R)\\ \mathbf{p}_I^{l+1}=(\rho+\frac{\rho}{2}\mathbf{b}_I^T\mathbf{b}_I)^{-1}(\frac{1}{4M}\mathbf{b}_I+\rho\mathbf{z}_I^l+\lambda_I^l+\frac{(\rho\alpha^l+\tau_\alpha^l)}{2}\mathbf{b}_I)\\ t^{l+1}=z_{n+1,n+1}^l+(\Lambda_{n+1,n+1}^l-\gamma)/\rho\\ \mathbf{u}^{l+1}=\mathbf{W}(\mathbf{T}^*(\mathbf{Z}_0^l+\mathbf{\Lambda}_0^l/\rho)-\frac{\gamma}{\rho}\mathbf{e}_1).\end{cases} \tag{18}$$

where $\mathbf{b}_R=\mathbf{\Gamma}^T\mathbf{y}_R$ and $\mathbf{b}_I=\mathbf{\Gamma}^T\mathbf{y}_I$ respectively. $\mathbf{W}$ is a diagonal matrix which is expressed as,

$$\mathbf{W}=\text{diag}\{[\frac{1}{N},\frac{1}{2(N-1)},\frac{1}{2(N-2)},\ldots,\frac{1}{2}]^T\}. \tag{19}$$

and $\mathbf{T}^*(\cdot)$ is the Toeplitz adjoint operator.

The matrix $\mathbf{Z}$ is a positive semidefinite one, and it can be calculated by

$$\mathbf{Z}^{l+1}=\left[\begin{bmatrix}\mathbf{T}(\mathbf{u}^{l+1}) & \mathbf{p}_R^{l+1}+j\mathbf{p}_I^{l+1}\\ (\mathbf{p}_R^{l+1}+j\mathbf{p}_I^{l+1})^H & t^{l+1}\end{bmatrix}-\frac{\mathbf{\Lambda}^l}{\rho}\right]_+. \tag{20}$$

In order to ensure the characteristic of positive semidefinite, we utilize a projection function $[.]_+$ to enforce the matrix onto the positive definite cone by performing an eigenvalue decomposition and setting all negative eigenvalues to zero.

At last, the dual variable α in (15) can be updated with the closed-form as below,

$$\alpha^{l+1}=\left[1-\left\langle\mathbf{y},\mathbf{\Gamma}\mathbf{p}^{l+1}\right\rangle_R-\frac{\tau_\alpha^l}{\rho}\right]_+, \tag{21}$$

where $\mathbf{p}^{l+1}=\mathbf{p}_R^{l+1}+j\mathbf{p}_I^{l+1}$. Regarding the dual variables, they can be updated with iterating rules,

$$\begin{cases}\mathbf{\Lambda}^{l+1}\leftarrow\mathbf{\Lambda}^l+\rho\left(\mathbf{Z}^{l+1}-\begin{bmatrix}\mathbf{T}(\mathbf{u}^{l+1}) & \mathbf{p}_R^{l+1}+j\mathbf{p}_I^{l+1}\\ (\mathbf{p}_R^{l+1}+j\mathbf{p}_I^{l+1})^H & t^{l+1}\end{bmatrix}\right)\\ \tau_\alpha^{l+1}\leftarrow\tau_\alpha^l+\rho(\alpha^{l+1}-1+\mathbf{y}_R^T\mathbf{\Gamma}\mathbf{p}_R^{l+1}+\mathbf{y}_I^T\mathbf{\Gamma}\mathbf{p}_I^{l+1})\end{cases} \tag{22}$$

After determining the noiseless measurement $\mathbf{p}$, the existing approaches utilize subspace-based methods, viz. MUSIC, to estimate DOAs via spectrum searching, which is not computationally efficient.

C. Effective Dual Polynomial Method for DOA Estimation

Next, different from the existing works using the noiseless measurement $\mathbf{p}$, we propose an effective dual polynomial method based on the estimate of α for DOA estimation. Towards this end, (10) is rewritten as,

$$\begin{aligned}\min_{\mathbf{p}_R,\mathbf{p}_I} \quad & -\frac{1}{2M}(\mathbf{y}_R^T\mathbf{\Gamma}\mathbf{p}_R+\mathbf{y}_I^T\mathbf{\Gamma}\mathbf{p}_I)+\gamma\|\mathbf{p}\|_\mathcal{A}\\ \text{s.t. } & \mathbf{y}_R^T\mathbf{\Gamma}\mathbf{p}_R+\mathbf{y}_I^T\mathbf{\Gamma}\mathbf{p}_I\leq 1.\end{aligned} \tag{23}$$

The Lagrange function of (23) is expressed as,

$$\begin{aligned}\mathcal{L}(\mathbf{p}_R,\mathbf{p}_I,\alpha)=\ &\gamma\|\mathbf{p}\|_\mathcal{A}-\frac{1}{2M}(\mathbf{y}_R^T\mathbf{\Gamma}\mathbf{p}_R+\mathbf{y}_I^T\mathbf{\Gamma}\mathbf{p}_I)\\ &+\alpha(\mathbf{y}_R^T\mathbf{\Gamma}\mathbf{p}_R+\mathbf{y}_I^T\mathbf{\Gamma}\mathbf{p}_I-1),\end{aligned} \tag{24}$$

with $\alpha\geq 0$. The dual function of (24) can be deduced via minimizing $\mathcal{L}$ with respect to $\mathbf{p}_R$ and $\mathbf{p}_I$,

$$\begin{aligned}g(\alpha)&=\inf_{\mathbf{p}_R,\mathbf{p}_I}\mathcal{L}(\mathbf{p}_R,\mathbf{p}_I,\alpha)\\ &=-\alpha+\inf_{\mathbf{p}_R,\mathbf{p}_I}(\gamma\|\mathbf{p}\|_\mathcal{A}+(\alpha\mathbf{y}_R^T\mathbf{\Gamma}-\frac{1}{2M}\mathbf{y}_R^T\mathbf{\Gamma})\mathbf{p}_R\\ &\quad+(\alpha\mathbf{y}_I^T\mathbf{\Gamma}-\frac{1}{2M}\mathbf{y}_I^T\mathbf{\Gamma})\mathbf{p}_I)\\ &=-\alpha+\inf_{\mathbf{p}_R,\mathbf{p}_I}(\gamma\|\mathbf{p}\|_\mathcal{A}-\left\langle(\frac{1}{2M}-\alpha)\mathbf{\Gamma}^T\mathbf{y}^*,\mathbf{p}\right\rangle_R)\\ &=-\alpha+I_{\{\omega,\|\omega\|_\mathcal{A}^*\leq\gamma\}}(\mathbf{q}),\end{aligned} \tag{25}$$

where $\mathbf{q}=(\frac{1}{2M}-\alpha)\mathbf{\Gamma}^T\mathbf{y}^*$, and $(\cdot)^*$ denotes the conjugate operator. The term $I_\mathcal{A}(.)$ is an indicator function which can be presented as,

$$I_{\{\omega,\|\omega\|_\mathcal{A}^*\leq\gamma\}}(\mathbf{q})=\begin{cases}0, & \|\mathbf{q}\|_\mathcal{A}^*\leq\gamma\\ -\infty, & \text{otherwise},\end{cases} \tag{26}$$

where $\|\cdot\|_{\mathcal{A}}^*$ is the dual atomic norm, defined as,

$$\|\mathbf{q}\|_{\mathcal{A}}^* = \sup_{\|\mathbf{p}\|_{\mathcal{A}} \le 1} \langle \mathbf{q}, \mathbf{p} \rangle_R = \sup_{\mathbf{a} \in \mathcal{A}} \langle \mathbf{q}, \mathbf{a} \rangle_R, \tag{27}$$

with $\langle \cdot \rangle_R$ as the real inner product. Thus the dual objective $g(\alpha)$ reaches its maximum $-\alpha$ if

$$\left\| (\frac{1}{2M} - \alpha) \mathbf{\Gamma}^T \mathbf{y}^* \right\|_{\mathcal{A}}^* \le \gamma. \tag{28}$$

Let $\hat{\mathbf{p}}$ be the optimal solution of (11), which can be decomposed as,

$$\hat{\mathbf{p}} = \sum_{k=1}^{K} c_k \hat{\mathbf{a}}(f_k), \tag{29}$$

where $\hat{\mathbf{a}}(f_k) \in \mathcal{S}$ with $\mathcal{S} \subset \mathcal{A}$ being regarded as the support of $\hat{\mathbf{p}}$. It is obvious that $\|\hat{\mathbf{p}}\|_{\mathcal{A}} = \sum |c_k|$. Since $\hat{\mathbf{q}} = (\frac{1}{2M} - \hat{\alpha}) \mathbf{\Gamma}^T \mathbf{y}^*$, based on (28), we have,

$$\langle \hat{\mathbf{q}}, \hat{\mathbf{p}} \rangle_R \le \|\hat{\mathbf{q}}\|_{\mathcal{A}}^* \|\hat{\mathbf{p}}\|_{\mathcal{A}} \le \gamma \|\hat{\mathbf{p}}\|_{\mathcal{A}}, \tag{30}$$

due to Hölder's inequality. On the other hand, from (25) and (26), we get,

$$\gamma \|\hat{\mathbf{p}}\|_{\mathcal{A}} - \langle \hat{\mathbf{q}}, \hat{\mathbf{p}} \rangle_R \le 0. \tag{31}$$

Combine (30) and (31), we obtain $\langle \hat{\mathbf{q}}, \hat{\mathbf{p}} \rangle_R = \gamma \|\hat{\mathbf{p}}\|_{\mathcal{A}}$, which indicates that $\hat{\mathbf{q}}$ and $\hat{\mathbf{p}}$ are primal-dual feasible. Therefore, we can conclude that $\langle \hat{\mathbf{q}}, \mathbf{a}(f_k) \rangle_R = \gamma$, for $\mathbf{a}(f_k) \in \mathcal{S}$, otherwise, $\langle \hat{\mathbf{q}}, \mathbf{a}(f_k) \rangle_R < \gamma$.

Note that the support set $\mathcal{S}$ is composed of the angular frequencies corresponding to DOAs. To the end, the angular frequency information can be extracted by the dual polynomial method as,

$$|\langle \hat{\mathbf{q}}, \mathbf{a}(f_k) \rangle_R| = \left| \sum_{n=0}^{N-1} q_n e^{j2\pi n f_k} \right| = \gamma. \tag{32}$$

Therefore, DOAs can be computed via inverse trigonometric function,

$$\hat{\theta}_k = \arcsin(2\hat{f}_k). \tag{33}$$

D. The Selection of Regularization Parameter

The choice of the regularization parameter plays an important role in the proposed method for DOA estimation. As analyzed in [17], [20], the regularization parameter γ is proportional to $\sqrt{\frac{\ln N}{M}}$, which can be expressed as $\gamma = C\sqrt{\frac{\ln N}{M}}$ with a scale factor C. Hence, an optimal C is the crucial factor for the accuracy of the proposed method. The experiment is conducted from varied scales of C to explore its relation with the reconstruction ratio $\tilde{r} = 10\log(\frac{\|\mathbf{p}\|_2^2}{\|\mathbf{p}-\hat{\mathbf{p}}\|_2^2})$ among 100 Monte Carlo trails, as shown in Fig. 2. From Fig. 2, we can see that the reconstruction ratio approaches its optimum when $C = 0.048$. In other words, the proposed method achieves the best estimation performance. This is a calibration process to settle the optimum regularization parameter, in the further simulations, γ is fixed as $0.048\sqrt{\frac{\ln N}{M}}$.

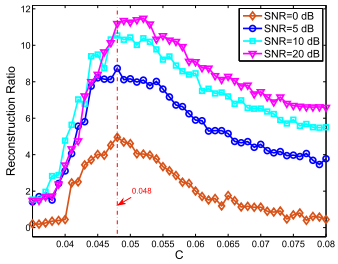

Fig. 2. The effect of the reconstruction ratio with C.

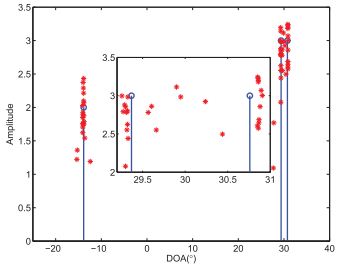

Fig. 3. The super resolution of the proposed method with closely-spaced sources.

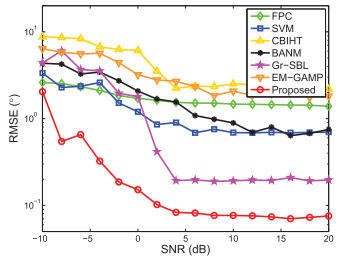

Fig. 4. RMSE versus SNR.

IV. Simulation Results

In this section, M elements of SLA are randomly sampled from the massive ULA with N sensors, where $M = 60$ and $N = 128$. All simulations in this letter are operated via Matlab 2014a on a PC platform with Windows 10 operation system. The signal-to-noise ratio (SNR) is defined as SNR $= 10\log\frac{\sigma_s^2}{\sigma_n^2}$. The root mean square error (RMSE) is commonly used to examine the performance of DOA estimation algorithms, which can be expressed as,

$$\text{RMSE} = \sqrt{\frac{1}{KP} \sum_{p=1}^{P} \sum_{k=1}^{K} (\hat{\theta}_{k,p} - \hat{\theta}_k)^2}, \tag{34}$$

where P denotes the number of the Monte Carlo runs and $\hat{\theta}_{k,p}$ is the DOA estimation of $\hat{\theta}_k$ at pth Monte Carlo run.

In the first experiment, three uncorrelated sources with directions from $\{-13.8597, 29.3692, 30.7596\}$ are considered to evaluate the effectiveness of the proposed method, where the last two sources are closely-spaced and SNR $= 10$dB. To investigate the proposed method being robust against the sign inconsistency, the signs of 6 elements in the measurements are chosen to flip. As seen in Fig. 3, it is observed that the proposed method can estimate DOAs accurately, where 15 Monte Carlo runs are considered. Fig. 4 illustrates the RMSE comparison versus SNR of the CBIHT [10], SVM [11], FPC [12], Gr-SBL [13], EM-GAMP [14], BANM [15], and the

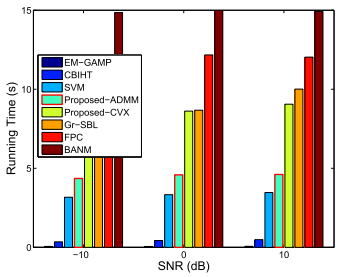

Fig. 5. The histogram of CPU running time.

proposed method with SNR varied from -10dB to 20dB. Three uncorrelated targets are randomly chosen from -90° to 90°, but each of them are separated at least 1°. Still, the signs of 6 elements from 60 measurements are flipped. The simulation result is averaged among 200 Monte Carlo runs. In addition, the grid steps of the discretized dictionary used in Gr-SBL, CBIHT and FPC algorithms are 0.1°. We observe that the proposed method is superior to other compared approaches.

In the next simulation, we will analysis the computational complexity of each methods. From [10], the computational complexity of CBIHT is around $\mathcal{O}(MN)$. The computational complexity of SVM and FPC is about $\mathcal{O}(N^3)$ and $\mathcal{O}(n_{inner}n_{outer}MN_d^2)$ respectively, where N_d, n_{inner} and n_{outer} represent the numbers of overcomplete dictionary, inner and outer iterations. It is well known that CVX solvers always exploit the interior-point methods to solve amount of linear equations along with the Newton directions, hence the overall computational complexity is approximately $\mathcal{O}(N^{3.5})$ [22]. On the other hand, the most computational demanded operation in ADMM is eigen-decomposition in (20), thus the computational complexity is $\mathcal{O}((N+1)^3)$ which is smaller than that of CVX by an order of 1.5. Finally, the CPU running time of all test methods is compared in Fig. 5, where the results are averaged among 100 Monte Carlo runs. The proposed method outperforms the FPC and BANM in terms of computational complexity. In addition, we compare the running time of CVX solving the problem in (11), to show the computational efficiency of the proposed method with ADMM as the solver.

V. Conclusion

Consider the problems of off-grid mismatch and sign inconsistency of one-bit measurements, a robust and gridless one-bit DOA estimation algorithm via atomic norm denoising is proposed. By combining the atomic norm minimization and the linear loss function, we derived a convex signal reconstruction optimization problem, solved by the efficient ADMM. Then, the polynomial method is proposed for DOA estimation with closed-form solution. Numerous simulation results verify the superiority and effectiveness of the proposed scheme.

References

[1] R. Cao, B. Liu, F. Gao, and X. Zhang, "A low-complex one-snapshot DOA estimation algorithm with massive ULA," *IEEE Commun. Lett.*, vol. 21, no. 5, pp. 1071–1074, May 2017.

[2] Z. Wei, W. Wang, B. Wang, P. Liu, and L. Gong, "Effective direction-of-arrival estimation algorithm by exploiting Fourier transform for sparse array," *IEICE Trans. Commun.*, vol. 102, no. 11, pp. 2159–2166, Nov. 2019.

[3] Q. Liu, Y. Gu, and H. C. So, "DOA estimation in impulsive noise via low-rank matrix approximation and weakly convex optimization," *IEEE Trans. Aerosp. Electron. Syst.*, vol. 55, no. 6, pp. 3603–3616, Dec. 2019.

[4] Z. Wei, X. Li, B. Wang, W. Wang, and Q. Liu, "An efficient super-resolution DOA estimator based on grid learning," *Radioengineering*, vol. 28, no. 4, pp. 785–792, Dec. 2019.

[5] Q. Liu, H. C. So, and Y. Gu, "Off-grid DOA estimation with nonconvex regularization via joint sparse representation," *Signal Process.*, vol. 140, pp. 171–176, Nov. 2017.

[6] X. Huang and B. Liao, "One-bit MUSIC," *IEEE Signal Process. Lett.*, vol. 26, no. 7, pp. 961–965, Jul. 2019.

[7] C.-L. Liu and P. P. Vaidyanathan, "One-bit sparse array DOA estimation," in *Proc. IEEE Int. Conf. Acoust., Speech Signal Process. (ICASSP)*, Mar. 2017, pp. 3126–3130.

[8] P. T. Boufounos and R. G. Baraniuk, "1-bit compressive sensing," in *Proc. 42nd Annu. Conf. Inf. Sci. Syst.*, Mar. 2008, pp. 16–21.

[9] L. Jacques, J. N. Laska, P. T. Boufounos, and R. G. Baraniuk, "Robust 1-Bit compressive sensing via binary stable embeddings of sparse vectors," *IEEE Trans. Inf. Theory*, vol. 59, no. 4, pp. 2082–2102, Apr. 2013.

[10] C. Stockle, J. Munir, A. Mezghani, and J. A. Nossek, "1-bit direction of arrival estimation based on compressed sensing," in *Proc. IEEE 16th Int. Workshop Signal Process. Adv. Wireless Commun. (SPAWC)*, Jun. 2015, pp. 246–250.

[11] Y. Gao, D. Hu, Y. Chen, and Y. Ma, "Gridless 1-b DOA estimation exploiting SVM approach," *IEEE Commun. Lett.*, vol. 21, no. 10, pp. 2210–2213, Oct. 2017.

[12] X. Huang, P. Xiao, and B. Liao, "One-bit direction of arrival estimation with an improved fixed-point continuation algorithm," in *Proc. 10th Int. Conf. Wireless Commun. Signal Process. (WCSP)*, Oct. 2018, pp. 1–4.

[13] X. Meng and J. Zhu, "A generalized sparse Bayesian learning algorithm for 1-bit DOA estimation," *IEEE Commun. Lett.*, vol. 22, no. 7, pp. 1414–1417, Jul. 2018.

[14] L. Xu, F. Gao, and C. Qian, "Gridless angular domain channel estimation for mmWave massive MIMO system with one-bit quantization via approximate message passing," 2019, *arXiv:1909.10114*. [Online]. Available: http://arxiv.org/abs/1909.10114

[15] C. Zhou, Z. Zhang, F. Liu, and B. Li, "Gridless compressive sensing method for line spectral estimation from 1-bit measurements," *Digit. Signal Process.*, vol. 60, pp. 152–162, Jan. 2017.

[16] Y. Plan and R. Vershynin, "Robust 1-bit compressed sensing and sparse logistic regression: A convex programming approach," *IEEE Trans. Inf. Theory*, vol. 59, no. 1, pp. 482–494, Jan. 2013.

[17] L. Zhang, J. Yi, and R. Jin, "Efficient algorithm for robust one-bit compressive sensing," in *Proc. 31st Int. Conf. Mach. Learn. (ICML)*, Beijing, China, Jun. 2014, pp. 2400–2410.

[18] G. Tang, B. N. Bhaskar, P. Shah, and B. Recht, "Compressed sensing off the grid," *IEEE Trans. Inf. Theory*, vol. 59, no. 11, pp. 7465–7490, Nov. 2013.

[19] V. Chandrasekaran, B. Recht, P. A. Parrilo, and A. S. Willsky, "The convex geometry of linear inverse problems," *Found. Comput. Math.*, vol. 12, no. 6, pp. 805–849, Dec. 2012.

[20] B. N. Bhaskar, G. Tang, and B. Recht, "Atomic norm denoising with applications to line spectral estimation," *IEEE Trans. Signal Process.*, vol. 61, no. 23, pp. 5987–5999, Dec. 2013.

[21] S. Boyd, N. Parikh, E. Chu, B. Peleato, and J. Eckstein, "Distributed optimization and statistical learning via alternating direction method of multipliers," *Found. Trends. Mach. Learn.*, vol. 3, no. 1, pp. 1–122, 2010.

[22] Y. Wang and Z. Tian, "IVDST: A fast algorithm for atomic norm minimization in line spectral estimation," *IEEE Signal Process. Lett.*, vol. 25, no. 11, pp. 1715–1719, Nov. 2018.